Sleep modifies retinal ganglion cell responses in the normal rat

Robert Galambos[†‡], Orsolya Szabó-Salfay[§], Erzsébet Szatmári[§], Nóra Szilágyi[§], and Gábor Juhász[§]

[†]University of California, San Diego, CA 92093; and [§]Eötvös Loránd University,1088 Múzeum krt, 4/A, Budapest, Hungary

Contributed by Robert Galambos, December 12, 2000

Recordings were obtained from the visual system of rats as they cycled normally between waking (W), slow-wave sleep (SWS), and rapid eye movement (REM) sleep. Responses to flashes delivered by a light-emitting diode attached permanently to the skull were recorded through electrodes implanted on the cornea, in the chiasm, and on the cortex. The chiasm response reveals the temporal order in which the activated ganglion cell population exits the eyeball; as reported, this triphasic event is invariably short in latency (5–10 ms) and around 300 ms in duration, called the histogram. Here we describe the differences in the histograms recorded during W, SWS, and REM. SWS histograms are always larger than W histograms, and an REM histogram can resemble either. In other words, the optic nerve response to a given stimulus is labile; its configuration depends on whether the rat is asleep or awake. We link this physiological information with the anatomical fact that the brain dorsal raphe region, which is known to have a sleep regulatory role, sends fibers to the rat retina and receives fibers from it. At the cortical electrode, the visual cortical response amplitudes also vary, being largest during SWS. This well known phenomenon often is explained by changes taking place at the thalamic level. However, in the rat, the labile cortical response covaries with the labile optic nerve response, which suggests the cortical response enhancement during SWS is determined more by what happens in the retina than by what happens in the thalamus.

optic chiasm | 5-HT | efferent retinal innervation

We have been studying the visual system of normal, behaving rats stimulated by a light-emitting diode (LED) permanently attached to the skull (1, 2). The red LED flashes activate the entire retina from behind the eyeball and evoke responses at electrodes implanted on the corneal surface of the eye, in the optic chiasm, and at the cortical terminal of the pathway. The overall objective is to describe the ganglion cell volley the retina creates as it converts rod/cone photochemical information into its neuronal equivalents and to follow that neuronal activity as it moves past the chiasm electrode en route, mainly, to the lateral geniculate nucleus (LGN) and the cortex beyond.

We have reported already that optic nerve axons exit the eyeball in a rigidly prescribed order for about 300 ms after stimulus onset (1). These ganglion cell volleys, called A/B/C/histograms[¶] because of their triphasic waveform, are the inevitable product of rat retinas excited by full-field stimuli, and, we have argued, of human retinas as well. Here we compare the histograms of sleeping and waking (W) rats, show they are labile, and conclude that optic nerve modulation probably is controlled by the serotonin fibers known to reach the retina from the midbrain dorsal raphe nuclei. Finally, we show that the well known cortical response enhancement during SWS is the approximate mirror image of the enhanced ganglion cell histogram, and we discuss the significance of this fact.

Materials and Methods

Published details (1, 2) can be briefly summarized. Young male Wistar rats, under halothane anesthesia and in a stereotaxic device, are implanted with stainless steel electrodes on the cornea, over each visual cortex, and, for sleep-staging, over the parietal cortex. A pair of epoxy-coated tungsten wires bared at the tip are inserted into the optic chiasm, and a small, stainless steel plate, the indifferent electrode always used during recording, is inserted under the skin over the masseter muscle. Two small LEDs are attached permanently to the skull with dental cement, along with two plugs through which connections are made to the stimulating and recording apparatus.

Testing began a day or so after implantation and continued intermittently for as long as 4 months. Most animals survived for several weeks and were tested repeatedly while awake and asleep between about 9 a.m. and 5 p.m. During testing, they were dark-adapted in a small box with glass walls inside a large, light-tight and sound-deadened Faraday cage. Responses were amplified conventionally, delivered to a Cambridge Electronic Devices signal analysis system (Cambridge, U.K.) and averaged by using SIGNAL 1.82.

Sleep-State Definitions. Fig. 1 shows the brainwave electroencephalogram (EEG) and power spectra that define sleep states. Slow-wave sleep (SWS) is characterized by synchronized EEG showing high δ power below 5 Hz; REM by predominance of high theta (6–7 Hz) power; and W by low θ power, long periods of β frequency, and motor artifacts. We followed Gottesmann's (3) classification, but lack of space prevented adding electrodes needed to identify his second SWS state or to identify REM rapid- and no-eye movement epochs. W records were obtained during alert and active periods at least a few minutes after the rat awoke.

In all experiments the EEG was monitored continuously on an oscilloscope and LED flashes (usually 1 ms; $n = 25$ or more, separated by at least 3 s) were delivered manually during one of the EEG states defined in Fig. 1. Data were stored ordinarily as averages, which often took many minutes to collect as the rat cycled out of and back into the desired state. Noisy responses and those from transition or atypical sleep states were not included in the averages. To collect single traces for statistical and other manipulations, the moment of stimulus delivery was marked on the EEG paper record, and the sleep category of each response was identified later by offline examination of the EEG trace. Data analyses used original scripts written in MATLAB for the WINDOWS 5.1 software

Abbreviations: W, waking; SWS, slow-wave sleep; REM, rapid eye movement; LED, light-emitting diode; LGN, lateral geniculate nucleus; EEG, electroencephalogram; 5-HT, 5-hydroxytryptophan; VEP, visual cortical evoked potential.

[‡]To whom reprint requests should be addressed at: 8826 La Jolla Scenic Drive, La Jolla, CA 92037. E-mail: rgalambos@ucsd.edu.

[¶]*Webster's Third New International Dictionary* defines ''histogram'' as ''a graphical representation of a frequency distribution by means of rectangles whose widths represent the class intervals and whose heights represent the class magnitudes.'' Microelectrode physiologists use the term to cover single-unit interval and poststimulus latency distributions whereas others plot phase histograms, two-dimensional histograms, etc. We use the term here for the poststimulus time distribution, at the computer sampling rate, of the ion current amplitude a large number of axons produce as they sweep past a fixed electrode.

The publication costs of this article were defrayed in part by page charge payment. This article must therefore be hereby marked "*advertisement*" in accordance with 18 U.S.C. §1734 solely to indicate this fact.

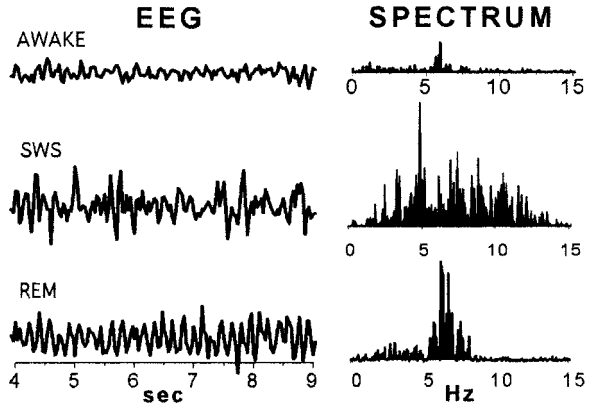

Fig. 1. Electrophysiological definition of rat sleep states. Typical EEG samples taken from a rat W, in SWS, and during REM (left), and the EEG power spectra of such samples (right). During online averaging, flashes were delivered manually only when the EEG pattern was seen to be consistent with one of these three brain states. In experiments where single responses were collected, the moment of stimulus delivery was marked on the EEG record, and each response was later classified as W, SWS, or REM when the EEG trace was examined.

environment (Mathworks, Natick, MA), and statistical calculations used the STATISTICA 5.1 (StatSoft, Tulsa, OK) program package.

Results

Fig. 2, which shows the results of two identical experiments performed 17 days apart on the same rat, illustrates the stability of the preparation, the validity of the sleep-staging procedures, and the lability of the optic nerve output. Each trace is the average of 100 LED flashes (n = 40 for REM) manually delivered only when the rat was judged by the EEG criteria to be W, in SWS, or in REM sleep. We recently published a detailed description of the phenomena seen in Fig. 2 and summarize it briefly here (1).

Optic Tract (Chiasm) Responses. The averaged responses in the middle column of Fig. 2 (chiasm) represent optic nerve activity that has reached the optic chiasm on its way to the LGN. Each individual response in the average is the neuronal equivalent of the photochemical information the rods and cones stored during a light flash. The typical end product, shown six times in Fig. 2, is a positive-negative-positive event lasting about 300 ms. We call these episodic phenomena histograms and label their three parts A/B/C/.

Rats have produced histograms to a wide range of stimuli varied in rate, luminance, and duration presented through either the pupil or the sclera during light- and dark-adapted states. Our earlier publication presented the evidence for this episodic view of the retinal neuronal output, compared it with the concepts based on conventional microelectrode studies, and suggested a way to reconcile them (1).

The rat A/B/C/histogram represents activity in a fraction of 110,000 ganglion cells of some 20 different types (4). A/signals the first axon departures at about 5 ms; it is rarely recorded at our standard chiasm electrode location, and does not appear in Fig. 2. The positive deflections B/and C/are separated by the negative deflection B− that, in every SWS record in this report, is deeper and wider during SWS than during W. B− often lacks a positive-going deflection (2B/) seen in W and REM traces. (We assume 2B/signals passage of an axon population that is not activated during SWS or is activated at a different time.) In short, we speculate that chiasm responses are labile because the retinal neuropile activates different groups of ganglion cells in sleeping and W rats. This lability, its possible physiological origins, and its significance for understanding the visual perceptual process are the topics of this paper.

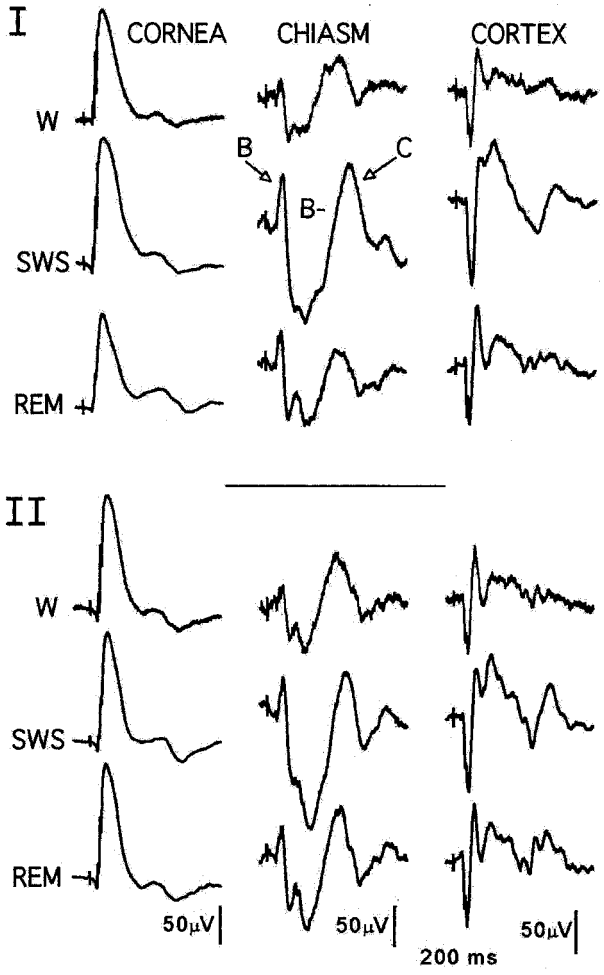

Fig. 2. Simultaneous retinal, optic tract, and visual cortical responses evoked during W and two stages of sleep. Stimuli (n = 50 or more) were 1-ms red flashes delivered through an LED attached to the skull. Data shown are replications 17 days apart on rat J25.

The Corneal and REM Traces. The most prominent feature of the six corneal traces in Fig. 2 is the electroretinogram b-wave, and the most notable facts about those b-waves are that they closely resemble each other but are not identical. SWS b-waves show no hint of the large chiasm changes recorded at the same time, which indicates the retina uses different mechanisms to generate its b-wave and ganglion cell outputs. Space limitations prevent further consideration of sleep b-waves here. The REM histograms are analyzed in a later section.

Statistical Examination of Sleep-Related A/B/C/Differences. Figs. 3 and 4 present the results of a statistical analysis of the differences between sleeping and W histograms. Five rats, instrumented as described by the same person (1), were tested between 9 a.m. and 5 p.m. after being dark-adapted for at least 30 min. Several days were required to collect the data from each rat. Individual responses to 1-ms LED flashes (luminance 5,500 lux) delivered at intervals of at least 3 sec were stored for later statistical manipulations and averaging. SWS and REM averages contain 50 such responses, but W responses often contain up to 100, because rats produce relatively noisy records when awake.

Fig. 3 presents the mean ± SD of the W, SWS, and REM histograms recorded from the five rats in the study. This figure contains all of the data used in the statistical analysis. In Fig. 4, the three mean histograms (W, SWS, and REM) of each rat are

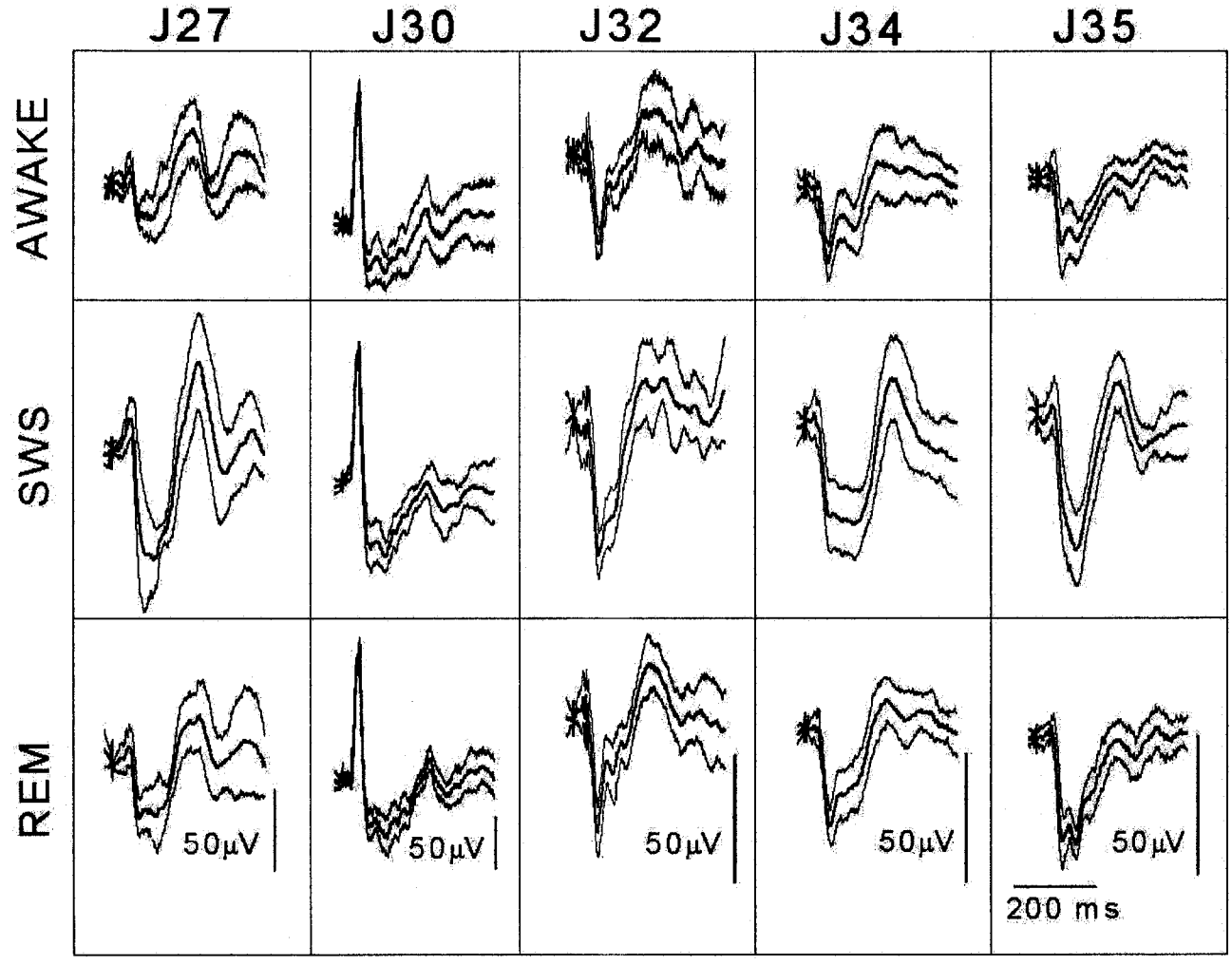

Fig. 3. Sleep/W data collected from five rats for statistical analysis. Each column shows, for one rat, the mean ± SD of the W, SWS, and REM histograms.

overlapped in the top row. (In these overlapped displays, the REM histogram can be identified because it always appears between the smaller W and the larger SWS histogram.) The area of each B/, B−, and C/deflection was then measured and plotted as a percentage of the waking results in the lower part of the figure. These areas are shown in the Fig. 4 *Inset* above and below the prolongation of the prestimulus baseline. A program written in MATLAB computed the region between this baseline and the response curve by numerical integration ($\mu V \times ms$).

After obtaining these areas, we used discriminant analysis and ANOVA to decide whether the five animals formed a homogenous group for B/, for B−, and for C/in SWS and in REM. J30 was an outlier for B/and C/(but not for B−) in both SWS and REM and was not included in the B/and C/calculations. The remaining four animals formed homogenous groups except for C/in REM, where we found two groups (J32, J35 and J27, J34). The differences in area were determined by using one-sample *t* tests after transforming the skewed distributions into normal distributions by a logarithmic transformation. The bar graphs compare the SWS and REM areas with the W area and give the significance of the B/, B−, and C/differences (***, $P < 0.001$; **, $P < 0.01$). C/areas increased significantly only during SWS for rat J34. The most important outcome of the analysis is that the increases in the B− area are highly significant during both REM and SWS for all animals.

Validation of the A/B/C/Histogram. Curiously, the five histogram patterns in Fig. 3 are about as different from the more usual A/B/C/pattern seen in Fig. 2 as any recorded from the 40 animals implanted with chiasm electrode during the past 2 years. The electrodes (approximately 100 μM of insulation removed above a 10-μM tip) were all aimed stereotaxically at a chiasm region where about 110,000 optic nerve fibers form a bundle approximately 2 mm by 0.5 mm in cross section (4). Histological sections through some of the electrode sites make clear what is intuitively obvious: two electrodes like ours never sample the same number and kind of ganglion cell axons.

Given such a recording situation, identical histograms recorded from two rats will be fortuitous. However, it should follow that the activity recorded at enough different electrode locations will contain all of the varieties of active ganglion cell axons the optic nerve contains. To test this idea, we show in Fig. 5*A* the grand average of the five different SWS patterns from Fig. 3 and the grand average of the two SWS histograms from Fig. 2. The match is good, which confirms the hypothesis that the average of a random sample will include all of the types (A/B/C/) a retina discharges into the optic nerve. Put another way, that neither trace in Fig. 5*A* displays A/, the rarely recorded units with minimum latencies around 5 ms (1, 5), does not mean the retina failed to create the entire A/B/C/sequence.

The Outlier, J30, Does Not Change in Sleep. When the J30 histogram, found to be deviant in the statistical analysis, was examined in detail, the surprising and informative fact illustrated in Fig. 5*B*

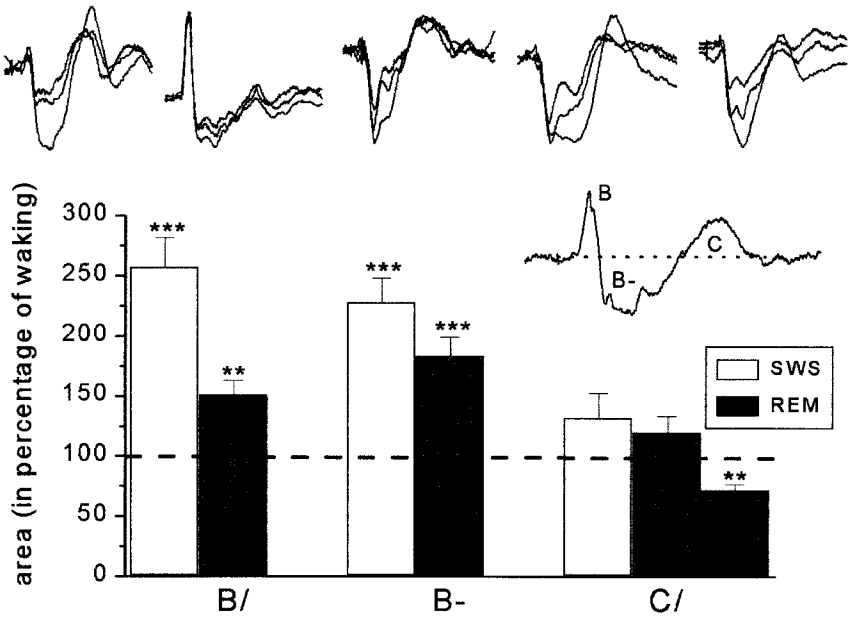

Fig. 4. Results of the statistical analysis. In the top row the W, REM, and SWS mean histograms for each rat in Fig. 3 are overlapped (in every case, the REM response lies between the W and SWS responses). (*Inset*) The three areas (B/, B−, and C/) that were measured and compared. The bar graphs give the percent difference between the sleep and W areas. During sleep, the increases in both the B/and B− areas of the histogram are highly significant for all animals.

emerged: at this electrode site, B/did not change when the rat fell asleep. Because four other rats showed highly significant sleep-related changes in B/(Fig. 4), it follows that at least two axon types contribute to the B/event—one of them changes its response during SWS, and the other does not. The abrupt appearance, at 60 ms, of sleep-dependent activity in Fig. 5*B* identifies still another feature of retinal responsivity for future research to examine. Perhaps the view of retinal activity a large electrode such as ours provides will uncover more unexpected details of the ways in which a retina responding to full-field flashes processes its bleached photoreceptor patterns.

The Special Case of REM. The three parts of Fig. 5*C* illustrate the variability of REM histograms. The *Upper* and *Lower* traces in each part are the same grand averages of a large number of W and SWS histograms obtained from rat J34. In the top group of histograms, the heavy trace, which lies about midway between the W and SWS traces, is the grand average of 11 individual REM averages from rat 34. In the middle group, the heavy line, which resembles the W trace, is the average of four REM traces. In the bottom group, the heavy line averages two REM traces and resembles the SWS trace. Obviously, the REM variability is large, but it rarely exceeds the limits set during the W and SWS states. A similar study (not shown) from rat J35 confirms that some REM histograms resemble W or SWS histograms, and some resemble neither of them. We have no explanation for this REM response variability.

Discussion

The optic chiasm measurement used in this study—the triphasic histogram (A/B/C/)—was described recently for the first time (1). Its heuristic value is demonstrated here by the fact that

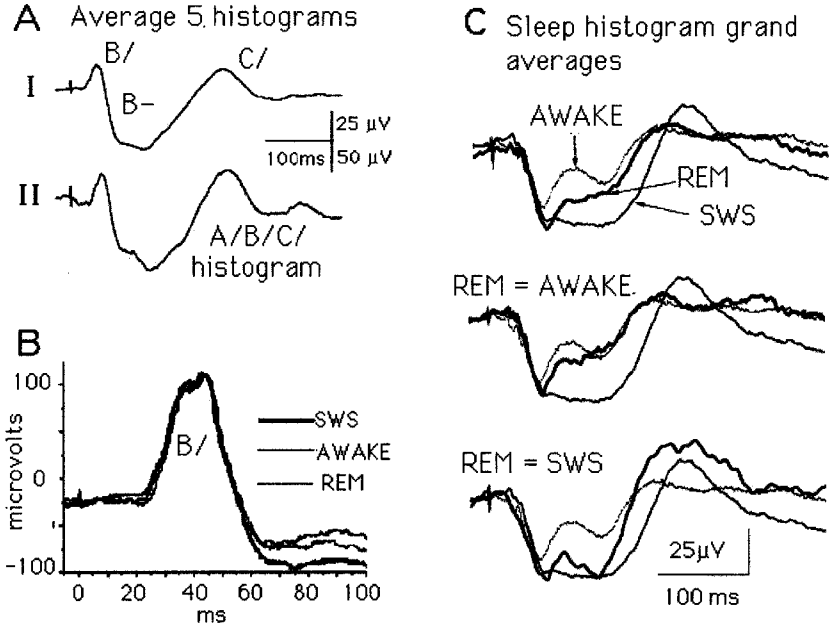

Fig. 5. Three examples of histogram variability. (*A*) The influence of the chiasm electrode location. Whereas none of the five SWS histograms in Fig. 3 looks like the "typical" triphasic A/B/C/histogram seen in Fig. 2, the grand average of the five histograms does. Explanation: at the electrode location where Fig. 2 was recorded, all of the axon types that leave the retina were sampled. Although this was not true at any of the five single sites, their grand average response indicates all of the fiber types were indeed sampled. (*B*) Some ganglion cells escape the 5-HT influences. At this electrode location, the statistically highly significant B/and early B− enhancements validated in Fig. 4 do not appear. Evidently, the ganglion cell population sampled by this electrode escaped the sleep-related changes under way elsewhere during the first poststimulus 60 ms. (*C*) REM histograms are variable. The three REM waveshapes (the heavy lines) are always located between the W and SWS waveforms, but one is near the W, another near the SWS, and the third lies between the two. This REM variability is unexplained.

histograms accurately and reliably identify sleep-dependent changes in retinal activity. Our literature search has not uncovered a prior claim that the rat retina invariably converts patterns of bleached photoreceptors into ganglion cell volleys lasting about 300 ms, nor have we found the claim that the pattern is labile (that it differs in sleeping and waking rats). It remains to be demonstrated, of course, how far these rat findings can be generalized to other mammals.

The strongest evidence for our sleep claim comes from the statistical analysis that confirms the enhancement of SWS histogram amplitude so evident to the eye in Fig. 2. The data (Fig. 3) and their analysis (Fig. 4) support the following assertions:

1. Reversible changes in the ganglion cell activity initiated by a flash of light take place as normal rats cycle between sleep and W.
2. When compared with the W, dark-adapted response, the SWS response is larger in amplitude and longer in duration during the 60 to 200-ms poststimulus interval.
3. Changes taking place before 60 ms and after 200 ms have not been defined clearly.
4. REM sleep changes can resemble the SWS changes but are usually smaller and more variable.
5. Minor sleep-related b-wave changes take place.
6. The visual cortical evoked potential (VEP) response covaries in amplitude and waveshape with an inverted version of its histogram.

The Serotonin Hypothesis. How can the fact a given stimulus produces different optic nerve outputs from sleeping and W rats be explained? In an earlier discussion of this problem (2), we identified the possible candidate mechanisms as humoral by way of the blood and neuronal through efferent fibers in the optic nerve; these new data favor the efferent neuronal explanation.

The catalogue of fibers reported to reach vertebrate retinas from various brain regions is surprisingly large [Ward *et al.* (6) list around 150 in their review]. Of all of these, we believe the serotonin fiber system is the most interesting possibility for explaining the rat phenomena. In their recent review of the neurotransmitter serotonin, Jacobs and Fornal (7) summarize its effects as follows (in part): "Brain serotonergic neurons display a distinctive slow and regular discharge pattern in behaving animals. This activity gradually declines across the arousal/W sleep cycle, becoming virtually silent during rapid eye movement sleep." We suggest the serotonin input to the retina varies similarly, and that during sleep its activity is negligible.

In 1984, Osborne (8) assembled information on the retinal distribution of serotonin (5-hydroxytryptophan, 5-HT) in vertebrates and pointed out that repeated searches for it in mammalian retinas had failed. By 1999, however, there were many reports that 5-HT neurons, which originate in the medulla and midbrain raphe region and send axons throughout the brain and spinal cord, also reach the mammalian retina (9–20). One negative report exists (21), and the reciprocal projection of retinal ganglion cell axons to the dorsal raphe nuclei has been reported twice (22, 23).

At least a dozen 5-HT receptor types are known (24), and four of these have been identified in the retina. Jin and Brunken (25) examined the distribution of 5-HT3, concluding the "serotoninergic system in retina (*i*) is associated specifically with rod-related pathways and (*ii*) exerts a powerful modulatory force over information transfer in the retina." Chidlow *et al.* (26) localized two different receptors, 5-HT1A and 5-HT7, in the ciliary process of the eye and found only 5-HT7 in the retina. Finally, Pootanakit *et al.* (27) found 5-HT2A immunoreactivity in both the inner and outer plexiform layers "on the terminals of photoreceptor and rod bipolar cells" and concluded that "serotonin may be a modulator of synaptic function in the retina." This sample of reports clearly supports the idea that several serotonin receptor types are involved in retinal neuropile activities.

We are not in a position to evaluate the accuracy of these anatomical and pharmacological claims. Taking them at face value, we propose that 5-HT input to the retina normally varies, as it does throughout the brain (7, 8), and that the input is larger or more effective during W. Presumably, serotonin input during wakefulness enables the activation of more ganglion cells, or perhaps the same number in a different sequence. During sleep, diminished 5-HT activities may prevent the retina from responding fully to its bleach patterns, and so its analysis of a scene (if the eyes were open) would in some way be incomplete. In short, we suppose the enhanced amplitude and duration of the SWS histogram measures change in the number, kind, or distribution of active ganglion cells. Interestingly, Fig. 5*B* makes it clear that if serotonin controls ganglion cell activities, some cells escape under some conditions.

To conclude, a strong presumption that serotonin is involved in retinal processing exists. Perhaps our functional evidence for sleep-related lability in the retinal output will encourage experiments that clarify the situation.

The Variable REM Response. That an REM histogram can resemble the W or SWS response, or neither of them (Fig. 5*C*), poses other interesting questions for future experiments. For example, 5-HT effects on the brain are said to be largest during REM sleep, but REM changes are almost always smaller and less stable in the retina. Perhaps the 5-HT input varies during REM, or the endogenous 5-HT receptors can act independently of efferent input. We have considered using 5-HT receptor agonists and antagonists to address such questions but suspect the information collected from freely moving rats would be difficult to interpret.

Finally, two REM states are recognized in many animals, one with dreaming, the other without. Perhaps the REM variability our experiments establish so securely is correlated with dreaming, strange as that may sound when rat brains are being discussed.

Expanding the View of Mammalian Retinal Functions. The evidence for efferents to the bird retina and the behavioral implications of that fact have been reviewed (e.g., ref. 28) and will not be examined here. Our previous review of the mammalian evidence (2) uncovered a claim that human optic nerve activity is modulated during selective attention (29), and another that it is not (30). However, the unexpected finding of labile rat optic nerve outputs prompted a broader literature search for evidence that mammalian retinas do more than passively transduce bleached photoreceptor patterns into ganglion cell discharges. Here we describe two reports that suggest the reversible reorganizations rat retinas undergo during sleep are not the only brain-like activity this unique structure displays.

Isolated Retinas. For many years Niemeyer and Kueng (31) placed a cat or dog eyeball in a heated box, perfused it for hours, stimulated it with light flashes, and recorded b-waves and optic nerve responses from it . The b-waves these isolated retinas produce resemble rat b-waves, but the optic nerve records do not resemble rat A/B/C/sequences at all. Niemeyer's (32) classical first report shows a single large spike followed by a flat elevated baseline for the duration of the stimulus. An obvious conclusion is that isolated eyeballs, which surely lack any serotonin input from the dorsal raphe nuclei, are also deprived of other input or inputs, neuronal, humoral, or both, that normally control ganglion cell activities. Whether the absence of efferent input is in fact responsible for the limited responses of isolated eyeball preparations is an open question.

In a different series of experiments, T. H. Bullock and his colleagues have studied temporal conditioning in the visual systems of invertebrates and vertebrates, including humans. In a typical

experiment, a fish optic nerve *in situ* responds to a brief series of flashes delivered at the rate of several hertz. When the flashes stop, a response appears with a latency correct for the stimulus that would have been delivered next but was not (33). Remarkably, fish eyeballs produce these omitted stimulus potentials (OSP) after the optic nerve is cut. Human brains produce OSPs also. The authors carefully distinguish these from P300 waves and think it probable that human OSPs, like those of the fish, originate at the retinal level (34). That isolated retinas acquire, store, deliver, and "forget" information about environmental events indicates that when the primordial retinal neuropile moves away from the forebrain during embryology, it brings along the capacity to create and deliver complex, brain-like integrative functions. Defining the number and variety of these functions has apparently only just begun.

The Retinal Origin of the VEP Response. We have proposed that the visual perceptual process begins when the retina creates an accurate neuronal version of the scene several times each second and ends after the brain processes these (1). The data reported here are consistent with this hypothesis. Sleeping and W rats create about 300-ms ganglion cell volleys, and the VEPs these generate resemble phase-inverted versions of them (Fig. 2). To reproduce at the cortex the exact temporal order in which the ganglion cell axons left the retina would seem to require at the LGN level the monosynaptic transfer the anatomists have long recognized could be the rule (e.g., refs. 35–37). From now on, speculations about how the rat visual system converts photoreceptor bleach patterns into visual perceptions must include the fact that, thanks to monosynaptic transfer at the LGN level, its cortex receives precise information about the sequence in which the ganglion cell axons left the retina.

Our facts are not in harmony with some existing concepts of the brain changes associated with sleep. It is common knowledge that VEPs are enhanced during sleep (Fig. 2), and this fact is attributed widely to neuronal events taking place at the thalamic level (e.g., ref. 38). However, to say transfer through LGN is monosynaptic is another way to say the various cortical, reticular, and brainstem inputs to LGN are inactive. The mirror-image relationship denoting monosynaptic transfer is still recognizable during W but it is less obvious, which suggests the LGN inputs are now active. During REM, as noted, the sleep-related facts are not yet entirely clear. The available evidence is consistent, then, with the view that, during SWS, LGN transfers its input from retina to cortex with minimal change (i.e., the transfer is mainly monosynaptic), and that during REM and wakefulness monosynaptic transfer is still the rule, but various polysynaptic processes are added. It is interesting and perhaps important to note that the input to LGN includes 5-HT axons (37).

In summary, we need to learn more about (*i*) the high inverse correlation between histogram and VEP waveshapes, and (*ii*) the influence of behavioral states such as sleep at all levels of the visual system from retina to cortex. Above all, we do not understand the mechanism that arranges the departure, three times each second, of tens of thousands of retinal ganglion cell axons in exactly the order that, for some unknown reason, is optimal for visual perceptions.

We thank T. H. Bullock, G. Niemeyer, and Walter Sannita for helpful discussions and Péter Barabás and János Pálhalmi for technical assistance. This work was supported in part by Hungarian Science Foundation Grant OTKA 628.

1. Galambos, R., Szabó-Salfay, O., Barabás, P., Pálhalmi, J., Szilágyi, N. & Juhász, G. (2000) *Proc. Natl. Acad. Sci. USA* **97,** 13454–13459. (First Published November 14, 2000; 10.1073/pnas.240448697)
2. Galambos, R., Juhász, G., Kékesi, A. K., Nyitrai, G. & Szilágyi, N. (1994) *Proc. Natl. Acad. Sci. USA* **91,** 5153–5157.
3. Gottesmann, C. (1992) *Neurosci. Biobehav. Rev.* **16,** 31–38.
4. Paxinos, G. (1995) *The Rat Nervous System* (Academic, San Diego), 2nd Ed. pp. xvii, 1136.
5. Yonemura, D. & Tsuchida, Y. (1968) *Jpn. J. Physiol.* **18,** 703–722.
6. Ward, R., Reperant, J. & Micili, D. (1991) in *The Changing Visual System*, eds. Bagnoli, P. & Hodos, W. (Plenum, New York), pp. 61–76.
7. Jacobs, B. L. & Fornal, C. A. (1999) *Neuropsychopharmacology* **21,** 1S–15S.
8. Osborne, N. N. (1984) in *Retinal Research*, (Pergamon, Oxford) 3rd. Ed., pp. 61–103.
9. Itaya, S. K. (1980) *Brain Res.* **201,** 436–441.
10. Itaya, S. K. & Itaya, P. W. (1985) *Brain Res.* **326,** 362–365.
11. Labandeira-Garcia, J. L. (1988) *Neurosci. Res. (N.Y.)* **6,** 88–95.
12. Labandeira-Garcia, J. L., Guerra-Seijas, M. J., Gonzalez, F., Perez, R. & Acuna, C. (1990) *Neurosci. Res.* **8,** 291–302.
13. Larsen, J. N. & Moller, M. (1987) *Exp. Eye Res.* **45,** 763–768.
14. Larsen, J. N. & Moller, M. (1985) *Acta Ophthalmol. Suppl.* **173,** 11–14.
15. Lima, L. & Urbina, M. (1998) *Neurochem. Int.* **32,** 133–141.
16. Schütte, M. (1995) *Visual Neurosci.* **12,** 1083–1092.
17. Villar, M. J., Vitale, M. L. & Parisi, M. N. (1987) *Neuroscience* **22,** 681–686.
18. Wolter, J. R. (1978) *Trans. Am. Ophthalmol. Soc.* **76,** 140–155.
19. Wolter, J. R. (1979) *Albrecht von Graefes Arch. Klin. Exp. Ophthalmol.* **210,** 31–41.
20. Bons, N. (1987) *C. R. Seances Soc. Biol. Fil.* **181,** 274–281.
21. Schnyder, H. & Künzle, H. (1984) *Exp. Brain Res.* **56,** 502–508.
22. Shen, H. & Semba, K. (1994) *Brain Res.* **635,** 159–168.
23. Kawano, H., Decker, K. & Reuss, S. (1996) *Neurosci. Lett.* **212,** 143–146.
24. Mann, J. J. (1999) *Neuropsychopharmacology* **21,** 99S–105S.
25. Jin, X. T. & Brunken, W. J. (1998) *Visual Neurosci.* **15,** 891–902.
26. Chidlow, G., Le Corre, S. & Osborne, N. N. (1998) *Neuroscience* **87,** 675–689.
27. Pootanakit, K., Prior, K. J., Hunter, D. D. & Brunken, W. J. (1999) *Visual Neurosci.* **16,** 221–230.
28. Woodson, W., Shimizu, T., Wild, J. M., Schimke, J., Cox, K. & Karten, H. J. (1995) *J. Comp. Neurol.* **362,** 489–509.
29. Eason, R. G., Oakley, M. & Flowers, L. (1983) *Physiol. Psychol.* **11,** 18–28.
30. Mangun, G. R., Hansen, J. C. & Hillyard, S. A. (1986) *Psychophysiology* **23,** 156–165.
31. Niemeyer, G. & Kueng, N. (1998) *Documenta Ophthalmologica* **95,** 55–61.
32. Niemeyer, G. (1981) *J. Neurosci. Methods* **3,** 317–337.
33. Bullock, T. H., Hofmann, M. H., Nahm, F. K., New, J. G. & Prechtl, J. C. (1990) *J. Neurophysiol.* **64,** 903–914.
34. Bullock, T. H., Karamürsel, S., Achimowicz, J. Z., McClune, M. C. & Basar-Eroglu, C. (1994) *Electroencephalogr. Clin. Neurophysiol.* **91,** 42–53.
35. Glees, P. (1961) in *The Visual System: Neurophysiology and Psychophysics*, eds. Jung, R. & Kornhuber, H. (Springer, Berlin), pp. 104–110.
36. Rodieck, R. W. (1998) *The First Steps in Seeing* (Sinauer, Sunderland, MA), p. 562.
37. Sherman, S. M. & Guillery, R. W. (1996) *J. Neurophysiol.* **76,** 1367–1395.
38. Steriade, M. & Llinás, R. R. (1988) *Physiol. Rev.* **68,** 649–742.